MAIT cells have a negative impact on GBM

Seketoulie Keretsu[1,*], Taijun Hana[1,*], Alexander Lee [2, 3], Hye Kim[1], Guzal Khayrullina[1], Ayaka Hara[1], Morgan Coombs[1], Matthew Watowich[1], Ananth Hari[4], Michael K.B. Ford[4], Cenk Sahinalp[4], Masashi Watanabe[1], Mark R. Gilbert[1], Robert Prins[2, 3], Masaki Terabe[1]

[1]Neuro-Oncology Branch, Center for Cancer Research, National Cancer Institute, National Institutes of Health, NIH, USA, [2]Department of Neurosurgery, UCLA, USA, [3]Parker Institute for Cancer Immunotherapy, [4]Cancer Data Science Laboratory, Center for Cancer Research, National Cancer Institute, National Institutes of Health, Bethesda, MD, USA

* These authors contributed equally

Running title:

MAIT cells have a negative impact on GBM

Corresponding:

Masaki Terabe, Ph.D, Neuro-Oncology Branch, National Cancer Institute, NIH, Building-37, Room-1016, 37 Convent Drive, Bethesda, MD 20892, USA

Tel: 240-760-6731

E-mail: terabe@mail.nih.gov

Funding: This work was supported in part by the intramural program of the National Institutes of Health, National Cancer Institute, Center for Cancer Research (ZIA BC 011877). R. Prins and A. Lee were supported in part by NIH/NCI grants (R01CA222695, R01 CA267726), the UCLA SPORE in Brain Cancer (P50CA211015), and the Parker Institute for Cancer Immunotherapy.

Conflict of Interest: The authors have no conflicts of interest to declare.

Keywords: Glioblastoma, MAIT cell, neutrophil, MDSC

Abstract:

Glioblastoma (GBM) is the most aggressive primary brain cancer without a cure and with a poor response to currently available immunotherapies. To delineate the role of Mucosal-associated invariant T (MAIT) cells in GBM, we analyzed GBM patient blood and tissue samples and multi-omic datasets. In bulk RNA sequencing data of cancer tissues, MAIT cell signature genes significantly correlated with poor patient survival, suggesting an immunosuppressive role of MAIT cells. In scRNA-seq data of $CD45^+$ cells from 23 GBM tissue samples, 15 (65.2%) were positive for MAIT cells. Clustering analysis showed that most MAIT cells belong to a Th17-like memory T cell cluster, indicating the skewed function of MAIT cells to IL-17 production. The MAIT cell signature significantly correlated with the activity of tumor-associated neutrophils (TANs)/myeloid-derived suppressor cells (MDSCs). Interestingly, genes involved in IL-17-mediated recruitment of neutrophils/MDSCs were upregulated in MAIT-positive patients. Indeed, multiple immune suppressive genes known to be used by TANs/MDSCs were upregulated in MAIT-positive patients. These results suggested that MAIT cells within the GBM tissue play an immunosuppressive role in driving the progression of GBM tumors through an IL-17-mediated induction of TAN/MDSCs. This MAIT-TAN/MDSC pathway gene expression showed a negative correlation with patient survival in other cancer types. Identifying this immune-suppressive pathway opens avenues for developing therapeutic strategies to disrupt a MAIT-TAN/MDSC axis.

Introduction

GBM is the most aggressive primary brain tumor, and its recurrence after primary treatment is inevitable despite the aggressive standard of care, including surgical resection followed by radiochemotherapy[1,2]. The five-year survival of GBM is approximately 5%, underscoring the urgent need for better treatment[3]. Immunotherapies have shown promise in treatments for other cancer types, but to date, have not shown clinical efficacy with GBM yet[4]. This lack of efficacy has been attributed to multiple factors, including a highly immunosuppressive microenvironment, which includes a high content of immunosuppressive myeloid cells[5]. However, factors that induce those immunosuppressive myeloid cells still require further investigation.

Recently, it was reported that a transcriptomic expression level of major histocompatibility complex class I-related (*MR1*) significantly correlated to the poor survival of glioma patients[6]. However, the underlying mechanism by which the *MR1* expression level correlates with poor survival still needs to be fully determined. MR1 is a non-classical MHC molecule that has been shown to present riboflavin derivatives; however, the repertoire of antigens presented is not well understood. It was recently reported that MR1 might load undefined cancer-derived antigens[7] More recently, nucleobase adducts were shown to be presented by MR1[8]. MR1 presents antigens to mucosal-associated invariant T (MAIT) cells, which express a semi-invariant TCRα chain utilizing the TCR gene segment combinations Vα7.2-Jα33, Vα7.2-Jα12, or Vα7.2-Jα20 in humans[7]. They are prevalent not only in mucosal tissues but also in non-mucosal tissues. Particularly, MAIT cells are highly prevalent in humans. MAIT cells secrete multiple cytokines, such as Th1 and Th17-cytokines, upon their activation. Their cytokine profile can be modified depending on the environment they are in[9]. In humans, MAIT cells have two functional subsets, IFN-γ-producing MAIT1 and IL-17-producing MAIT17. Most of the MIAT cells in tissues are

capable of producing IL-17[10-12]. Th17-type cytokines promote the local attraction and activation of specific myeloid cells, such as neutrophils, through the induction of chemokines[13,14].

The role of MAIT cells in cancer immunity is unclear[9]. MAIT cells can potentially lyse cancer cells, including glioma-derived cells, under certain in vitro conditions, but their ability to target cancers in vivo has not been confirmed[15,16]. They were reported to facilitate tumor immunity in liver cancer models when stimulated with CpG + 5-OP-RU, MAIT cell agonist[17]. However, they were shown to be suppressed by myeloid cells in tumor tissue[18]. On the other hand, MAIT cells promoted tumor growth and metastasis in mouse tumor models[16,19]. An inverse correlation between the number of MAIT cells in cancer tissues and patient survival has been reported in liver and colorectal cancer[20,21]. The discrepancy in the role of MAIT cells among tumor immunological studies suggests that MAIT cell functions could be modified by their surrounding environment. The interaction between GBM and MAIT cells has yet to be well studied. An earlier study proposed the existence of MAIT cells in clinical GBM samples, but their clinical impact or function remained to be elucidated[22].

We explored the role of MAIT cells in GBM by using multi-omics and flow cytometry. By utilizing TCGA-GBM and CGGA datasets, we found a significant correlation between the expression levels of MAIT cell signature genes and GBM patients' poor survival. Patients with MAIT TCR transcripts showed a higher expression of *IL17A,* which could induce chemokines that recruit myeloid cells[23]. In a single-cell RNA-seq study of tumor-infiltrating leukocytes (TILs) from 23 patients, 15 patients (65%) were found positive for MAIT cells, accounting for 1.46% of all T cells. MAIT cells clustered with cell populations expressing a high level of transcription factor gene *RORC*, suggesting the potential of these cells to produce IL-17. Consistent with these observations, further analysis indicated that MAIT cells in GBM correlated

with the activity of TANs/MDSCs. Based on the findings, we propose a hypothesis that MAIT cells play a tumor-promoting role in GBM through the production of IL-17, which activates TANs/MDSCs.

Materials and Methods

The definition of GBM in this study

With WHO classification 2021, isocitrate dehydrogenase (IDH) mutant grade 4 astrocytoma was excluded from the previously defined "glioblastoma"[24]. However, after examining the data, we determined that dividing the grade 4 gliomas into multiple subtypes in our study was not essential. The role of MR1 and MAIT cells was considered to be consistent in high-grade gliomas. Therefore, our definition of GBM in this study is in line with the WHO-2016 definition. The disease concept is along with The Cancer Genome Atlas (TCGA)-GBM dataset, in which all GBMs represent the grade 4 gliomas of IDH mutant and wild type.

GBM patient tissue collection and single cell isolation

The UCLA Medical Institutional Review Board 2 (IRB#10-000655-AM-00059) approved all protocols related to patient tumor specimen collection at UCLA. All GBM patients (newly diagnosed and recurrent) were treated with standard-of-care therapies. All patients provided written informed consent, and this study was conducted under an institutional review board-approved protocol. Patients with recurrent GBMs who received neoadjuvant anti-PD1 therapy

were given an intravenous infusion of off-label, off-trial pembrolizumab 14 +/- 5 days before surgery, similar to a previously published study[25].

Tumor-infiltrating $CD45^+$ immune cell populations were isolated from GBM tumors of patients undergoing surgical resection at the University of California, Los Angeles. Resected tumor tissue not needed for diagnosis was digested using the Miltenyi Brain Tumor Dissociation kit (Miltenyi Biotec, cat. 130-095-42) and gentleMACS dissociator (Miltenyi Biotec, cat. 130-093-235). After treatment with Myelin Removal Beads II (Miltenyi Biotec, cat. 130-096-433) cells were labeled with $CD45^+$ microbeads (Miltenyi Biotec, cat. 130-045-801). $CD45^+$ cells were positively selected from the tumor digest with Miltenyi LS columns (Miltenyi Biotec, cat. 130-042-401) and MidiMACS separator (Miltenyi Biotec, cat. 130-042-302) and immediately frozen for batched analysis in Bambanker (Fisher Scientific, cat. 302-14681) and stored in liquid nitrogen.

Single cell library preparation and sequencing

On the day of single-cell library preparation, $CD45^+$ cells collected from GBM patient tumors, regardless of treatment and recurrence, were thawed, counted and resuspended in PBS with 0.4% BSA (Gemini, cat. 700-101P-100). Single-cell library construction was performed by the Technology Center for Genomics and Bioinformatics Core, UCLA, utilizing the Chromium single-cell 5′ and VDJ library construction (10x Genomics), per manufacturer's protocol. Sequencing of the constructed single-cell libraries was carried out on a Novaseq S4 2x100bp flow cell (Illumina).

Single-cell RNA-seq data processing and analysis

Data were demultiplexed and aligned with Cell Ranger version 7.1 (10X Genomics) and aligned to the Genome Reference Consortium Human Build 38 (GRCh38-2020). Quantification of transcripts was carried out using *cellranger count* with *--force-cells: 8000* and *--include-introns: true*. *CellRanger aggr* was used to aggregate the samples for downstream analysis. TCR transcripts were quantified using *cellranger vdj.* The quality-checking reports from Cell Ranger were analyzed to assess sequencing quality and determine cell and gene counts per sample. Single-cell sequencing data were analyzed in R using the *Seurat* pipeline[26]. The preliminary analysis was conducted for each sample to filter out empty cells and doublets. Cells with a minimum of 200 genes and genes with a minimum 20 cells were included for downstream analysis. Cells having a percentage of mitochondrial gene counts higher than 5% of total gene counts were also excluded. Normalization was performed with *NormalizeData* and with the normalization method set to *LogNormalize* and the scaling factor set to *1e6*. The gene expression values were scaled with *ScaleData* function with variables to regress accounting for mitochondrial features, ribosomal features, and cell cycle score. Principal component analysis (PCA) was performed using *RunPCA* with the number of principal components set to 50. The significance of the principal components was evaluated based on the 'scree test' method, and 30 principal components were selected. Sample integration was performed with *harmony*. Unsupervised clustering based on uniform manifold approximation and projection (UMAP) with 30 principal components was used to generate the clusters. The Seurat objects from the individual samples were integrated into one *Seurat* object.

Further analysis of the clusters was carried out by separating the cells of the clusters of interest and repeating the abovementioned analysis process. The *FindAllMarkers* function with default parameters (Wilcoxon Rank Sum test) was used to find the genes differentially expressed in each

cluster. Clusters were annotated based on marker genes reported in previous studies[27,28]. The TCR VDJ profile data were also integrated with the gene expression data in R based on the matching cell barcodes. MAIT cells were identified by the expression of the TCR *a*-chain gene segments *Va7.2* and *Ja33/Ja22/Ja12*.

Differential expression analysis

Differential expression analysis was performed using the bulk RNA-seq analysis pipeline, using limma, glimma, and edgeR, as described by Law et al., 2016 [29].

PBMC collection

Blood samples were collected from newly diagnosed GBM patients recruited as part of a clinical trial at the Neuro-Oncology Branch at the National Cancer Institute [NCT04817254]. GBM patients' blood-derived Peripheral blood mononuclear cells (PBMCs) were collected using CPT tubes (BD Vacutainer CPT with sodium citrate, #362761) and stored in a liquid nitrogen freezer until they were used for assays.

PBMCs from healthy donors were isolated from buffy coat samples obtained from the NIH Blood Bank using Ficoll-Paque Plus (Millipore Sigma). All patients and healthy donors signed an institutional review board – approved, written informed consent form for collection of blood samples.

PBMC Sample preparation and cytokine stimulation.

PBMC samples from healthy donors were obtained from the NIH Blood Bank. PBMC samples from GBM patients were obtained from clinical trial (*NCT04817254*). PBMCs were stimulated

as a single-cell suspension at a concentration of 4-5 x 10^6 cells/mL with the Cell Activation Cocktail (Biolegend, Cat # 423301) and incubated at 37°C with 5% CO_2. Brefeldin A was added after 1 hr, and cells were further incubated at 37°C with 5% CO_2 for an additional 5 hrs before the harvest for flow cytometry.

Flow cytometry

Approximately 2 x 10^6 cells per sample were stained with LIVE/DEAD™ Fixable Aqua Dead Cell Stain Kit according to manufacturer's instructions (Invitrogen LIVE/DEAD™ Fixable Aqua Dead Cell Stain Kit, for 405 nm excitation, Thermo Fischer) for 30 min at room temperature (RT) in the dark. Cells were then washed (5 min, 350 x *g*) with HBSS containing 0.1% bovine serum albumin and 0.05% sodium azide. Cells were subsequently incubated with a cocktail containing Human TruStainFcX (Biolegend) and PBS-57/CD1d-tetramers (NIH Tetramer Facility) for 20 mins and subsequently stained with the surface antibodies against CD3 (Biolegend cat #: 300324), CD4 (BD cat #:611887), CD8 (BD cat #: 563795), Vα7.2 (Biolegend cat #: 351730), CD161 (Biolegend cat #: 339916) (for 30 mins at 4°C. Cells were washed twice with HBSS containing 0.1% bovine serum albumin and 0.05% sodium azide. Intracellular cytokine staining (ICS) was performed according to manufacturer's instructions (Biolegend Cat#420801; Cat#421022), and stained with antibodies specific for IFN-γ (Biolegend cat #: 502538), TNF-α (Biolegend cat #: 502912), IL-4 (Biolegend cat #: 500818), and IL-17A (Biolegend cat #: 512322). Samples were analyzed using the Cytek®Aurora flow cytometer (Cytek Biosciences, Fremont, CA, USA).

Identification of MR1 mutational frequency, the epigenetic transcriptional status, and the transcriptional distribution in GBM tissue

The mutational frequency was confirmed using *cBioportal* (https://www.cbioportal.org/). A total of 3391 multi-grade glioma samples were examined. The H3K27ac ChIP data of GSM1824806/1824808 were used for the ChIP analysis. Single-cell RNA-sequencing (RNA-seq) analyzing web tool, GBM-seq, was used to generate the tSNE plot of *MR1* expression in GBM.

Examining correlation between MR1 and TRAV1-2 gene expression in scRNA-seq data from glioma patients

We analyzed the 10X Genomics 3' scRNA-seq dataset from Abdelfattah et al (2022)[30], who sequenced 44 tumor fragment samples from 18 patients with low-grade glioma, newly diagnosed GBM, and recurrent GBM (GEO: GSE182109). Out of the 201986 cell barcodes that pass quality control, the authors labeled 19570 of them to be T cells. From all samples' feature-barcode matrices output by *CellRanger*, we extracted the number of non-T cells expressing MR1 and the number of T cells expressing TRAV1-2 into two column vectors (Supplementary Table 10). We used the latter as a proxy for the count of MAIT cells since the expression of TRAJ12/33/20 could not be captured with the limited resolution of the 3' dataset. We then computed Spearman's rank correlation coefficient between the two vectors.

Gene expression analysis and the predictive examination for GBM and pan-cancer analysis

All bulk RNA-seq data analyzed in this study are in fragments per kilobase of transcript per million mapped fragments (FPKM) unit. The TCGA-GBM core 168 samples' (Supplementary Table 1) transcriptomic data was downloaded from the Genomic Data Commons Data Portal

(https://portal.gdc.cancer.gov/). All the transcriptomic analyses were conducted using this set of data. Prognostic examinations were done with the data of TCGA-GBM 153 samples (Supplementary Table 2) with available clinical data using the Log-rank test, and all cut-off thresholds were decided using TCGA survival data analyzer[31]. For TCGA pan-cancer analysis, transcriptomic/clinical data were obtained from The Human Protein Atlas[32]. When comparing specific gene expressions between two groups, a two-tailed unpaired Student's t-test was used, and $p < 0.05$ was considered significant. When fold changes in gene expression were calculated, the mean FPKM of both groups was used.

Chinese Glioma Genome Atlas (CGGA) data portal was used to analyze as well[33]. In the CCGA data analysis, we integrated the datasets (mRNAseq_693 and mRNAseq_325) and the samples were filtered to include only primary, IDH-wildtype and MGMTp un-methylated glioblastoma patients. The expression values were normalized using *edgeR* in R. Outliers datapoints were removed by eliminating data below Q1 - 1.5*IQR or above Q3 + 1.5*IQR where, IQR is the interquartile range and Q1 and Q3 are quartiles.

Analyses using the signature of neutrophil degranulation and MDSC

The signatures/indexes of Neutrophil degranulation, and MDSC were defined based on a public database and previous studies of MDSC[34] and Treg[35]. The signature genes are provided in Supplementary Table 3.

Detecting the MAIT-positive samples in TCGA-GBM

All FASTQ files were downloaded from the GDC-Data Portal Legacy Archive (https://portal.gdc.cancer.gov/legacy-archive/). Reads with the characteristic T cell receptor

sequences (Supplementary Table 4) of MAIT cells were searched with the FASTQ files. The samples containing the reads of TRAV1-2(Vα7.2) and TRAJ33(Jα33) or TRAJ12(Jα12) or TRAJ20(Jα20) were classified as the samples with the MAIT cell infiltration and were defined as MAIT-positive. The MAIT-infiltration level of each sample was calculated with the formula given below:

$$MAIT\ infiltration\ level = \frac{(detected\ read\ count\ of\ the\ TRAV_{1-2}\ of\ the\ sample)}{(total\ RNA\ read\ count\ of\ the\ sample)}$$

All these analyses were conducted on the NIH-high performance computer, the Biowulf cluster system.

Gene expression heatmap and Gene Set Enrichment Analysis (GSEA)

GSEAs of this study were conducted using the expression data of core 168 TCGA-GBM samples and the pan-cancer samples.

Ethics

Access to TCGA-controlled data and studies using them were approved by the National Cancer Institute (#28406).

Data availability

The TCGA-GBM and CCGA data used in this study are publicly available. The glioblastoma TCGA data can be downloaded from https://www.cbioportal.org/. The CCGA dataset can be downloaded from http://www.cgga.org.cn/.

Results

MAIT cells decreased in peripheral blood in GBM patients

To investigate if MAIT cells change in quantity and quality in GBM patients, we quantified the MAIT cells ($V\alpha7.2^{+}CD161^{+}$ T cells) in the peripheral blood of GBM patients by flow cytometry. We compared them with the MAIT cells in the peripheral blood from healthy donors. The frequency of circulating MAIT cells among T cells in GBM (median % of total T cells = 0.45%) was significantly lower than that of the healthy controls (median % of total T cells = 2%), suggesting a preferential reduction of MAIT cells in the circulation of GBM patients (Figure 1A). To examine the functions of MAIT cells, PBMCs were stimulated with PMA and ionomycin and stained for TNF-α, IL-17, IFN-γ, and IL-4. We could not detect any IL-4-producing MAIT cells. The frequencies of MAIT cells that are single producer of IFN-γ or TNF-α ($IFN\text{-}\gamma^{+}IL\text{-}17^{-}TNF\text{-}\alpha^{-}$ or $IFN\text{-}\gamma^{-}IL\text{-}17^{-}TNF\text{-}\alpha^{+}$) were significantly higher in the healthy donor samples than in the GBM patients (Figure 1B). Interestingly, the frequencies of MAIT cells producing both IL-17 and IFN-γ were significantly higher in the GBM patients regardless of the TNF-α production status ($IFN\text{-}\gamma^{+}IL\text{-}17^{+}TNF\text{-}\alpha^{-}$ or $IFN\text{-}\gamma^{+}IL\text{-}17^{+}TNF\text{-}\alpha^{+}$). These results showed a decrease in circulating MAIT cells in GBM patients compared to healthy donors, as well as a tendency of patient MAIT cells to produce more IL-17.

MR1 expression levels correlated with worse overall survival in GBM patients

Since MAIT cells are considered to be tissue-resident cells, we focused our study on MAIT cells and their antigen-presenting molecule MR1 in GBM tissues. MR1 has been reported to be expressed in multiple cancer types, but the exact role of MR1 in cancer immunity is not well studied[6]. We analyzed the expression of MR1 at the genomic, transcriptomic and epigenomic

levels. Bulk transcriptomics data of GBM patients were collected from the TCGA[36] and CCGA database[33,37,38]. The samples' *MR1* expression levels in TCGA-GBM varied (Figure 1C). We then observed significant negative correlations between *MR1* expression levels and GBM survival using TCGA-GBM and CGGA data (Figure 1D & 1E), with higher expressions of *MR1* being associated with worse survival, in agreement with the previously reported prognostic value of *MR1* expression in glioma[6]. We also investigated whether the observed association could be attributed to functional mutations in *MR1* but found a very low frequency (0.06%) of genomic mutations in 3391 glioma samples, none of which had the reported loss of function mutation MR1-R31H21[39] (Figure 1F). Additionally, we found that the *MR1* promotor was active across GBM and grade 3 astrocytoma using H3K27ac ChIP data[40] (Figure 1G). Given the bulk tissue nature of TCGA-GBM samples, we considered whether the *MR1* expression in a subset of the samples could be due to the larger contribution of micro-environment components in those samples. We utilized single-cell RNA-seq data[41] and found that *MR1* was widely expressed in both glioma cells and TILs in GBM and that *MR1* expression was relatively upregulated in the tumor core compared to the tumor periphery (Figure 1H). We also performed a correlation analysis of the *MR1* with the *Vα7.*2, the gene segment of the TCR α-chain expressed by MAIT cells using a previously reported scRNA-seq data of glioma patient data[30]. The number of cells expressing the *Vα7.2* gene was adjusted based on the total number of T cells in the sample, and the number of cells expressing the *MR1* gene was adjusted based on the total number of non-T cells. *MR1* showed a moderate but significant correlation with *Vα7.*2 (correlation coefficient: 0.4, $p=0.0091$). All these observations indicated that intact *MR1* is widely transcribed in GBM tissue. A high expression of *MR1* was associated with poor prognosis in GBM patients. The underlying

mechanism regarding the high *MR1* expression and its clinical consequence in GBM tissues is unknown.

Expression levels of MAIT cell signature genes correlated with poor disease prognosis of GBM

MR1 is critical for the activation of MAIT cells. However, MR1 expression in GBM tumors is not direct evidence of MAIT cell activity because MR1 expression is necessary but not sufficient to prove MAIT cell activation. To understand the clinical significance of MAIT cells in GBM, we next conducted correlation analyses of MAIT cell signature genes *SLC4A10*, *CXCR4* and *MAF* and patient survival using TCGA-GBM and CCGA datasets. *SLC4A10, CXCR4* and *MAF* have been reported as markers for MAIT cells in recent transcriptomics studies[18,42-44]. Grouping of patient samples was performed by bifurcating the samples based on high or low expression of the MAIT signature genes. The expression level of *SLC4A10*, *CXCR4* and *MAF* showed a negative correlation with the probability of survival in GBM patients in both TCGA-GBM and CCGA datasets (Figure 1I-1N). These suggested that MAIT cells have a negative impact on the survival of GBM patients.

MAIT cells were identified in GBM patients

Since the information on MAIT cells in GBM tissues was minimal, we sought more direct evidence for MAIT cells with the TCGA-GBM dataset. To detect MAIT cells in bulk transcriptomic data, we took advantage of the expression of a unique semi-invariant TCR α-chain by MAIT cells (details are in Methods). MAIT cells specifically express the TCR α-chain using the Vα gene segment *Vα7.2 (TRAV1-2)* in combination with the Jα gene segment *Jα33 (TRAJ33),*

Jα20 (TRAJ20) or Jα12 (TRAJ12). The samples were bifurcated into MAIT-positive and MAIT-negative groups based on the positive/negative expression of the invariant TCRα-chain sequence in *Vα7.2 and Jα33/12/20* in the samples (Supplementary Table 4). Fourteen out of the 168 (8.3%) TCGA-GBM samples were identified as MAIT-positive (Figure 2A & Supplementary Table 1). We also evaluated the expression level of the MAIT cell signature genes *SLC4A10*, *CXCR4* and *MAF* in the MAIT-positive and -negative groups. The expression levels of *CXCR4* and *MAF* were significantly higher in the MAIT-positive samples. *SLC4A10* was not significantly different between MAIT-positive and negative groups. This may be because SLC4A10 was expressed in other non-MAIT cells (Supplementary material, Figure 1). We then evaluated the transcriptomic expression of the MAIT cell surface receptors, *CCR5*, *CCR6*, *CXCR6*, *CD161*, *IL-12R,* and *IL-18R*. All 6 genes had significantly higher expression levels in MAIT-positive samples (Figure 2B). The expressions of *IL17A*, *TNF*, and *IFNG*, typical cytokines secreted by MAIT cells, were also examined. The expression levels of *IL17A* and *TNF* were significantly higher in MAIT-positive samples. However, no difference in *IFNG* expression was detected (Figure 2C). These data supported our hypothesis that samples containing transcripts of the invariant TCRα gene segment were positive for MAIT cells. The cytokine gene expression data also raised the possibility that MAIT cells in GBM tissue may have a defect in producing IFN-γ.

The attributes of the MAIT-positive/negative samples were clarified as follows. Although there was no IDH mutant case in MAIT-positive samples, there was no statistically significant deviation in the distribution of the IDH mutant cases among the MAIT-positive/negative samples (Binomial test, $p = 1$). Other indicators also did not differentiate the MAIT-positive sample, and the MAIT-positive samples were statistically evenly distributed in multiple GBM subtypes[45] (Figure 2D & 2E). These findings indicate that MAIT cell infiltration is not significantly

associated with conventional attributes. We then examined the *MR1* expression status of MAIT-positive samples and found that MAIT-positive samples had a significantly higher expression level of *MR1* than MAIT-negative samples (Figure 2F). This important finding showed that the *MR1* as well as MAIT cell signature genes are highly expressed in MAIT-positive patients.

To further confirm the existence of MAIT cells in GBM tissues, we performed single-cell RNA sequencing (scRNA-seq) of FACS sorted $CD45^+$ leukocytes from 23 GBM patient samples to identify and characterize MAIT cells in GBM tumors. The GBM patient cohort comprised nine patients newly diagnosed with GBM, seven recurrent patients who have not been treated with any immunotherapy, and seven recurrent GBM patients who were treated with neoadjuvant anti-PD1 therapy (Supplementary Table 5). The $CD45^+$ leukocytes isolated from GBM tumor samples were applied for scRNA-seq and TCR VDJ sequencing. After a filtering process for quality assurance, a total of 89622 cells were used for further downstream statistical analysis. Initial clustering of the cells resulted in one lymphoid cluster, one myeloid cluster, and one cluster having Tumor/normal brain cells (Figure 3A & Supplementary material, Figure 5). The lymphoid cluster was positive for *CD3D/E/G*. The myeloid cell cluster showed high expression of myeloid cell makers, including *CD14*, *CD16, TMEM119* and *P2RY12,* and was negative for *CD3D/E/G* expression. One cluster was enriched in tumor and normal brain cell markers like *GFAP* and *SOX2*.

MAIT cells express many genes expressed in conventional T cells; hence, identifying them from a diverse population of T cells is challenging. However, using the TCR sequencing method, we were able to identify MAIT cells. We analyzed the TCR sequencing data of the 23 patients. MAIT cells were identified by the expression of semi-invariant TCR gene utilizing the combinations of *Vα7.2-Jα33, Vα7.2-Jα12, or Vα7.2-Jα20*. In the cohort of 23 GBM patients, 15

(65.2%) patient samples contained MAIT cells (Figure 3B). In MAIT-containing samples, we identified 89 MAIT cells (1.46% of total T cells) from a total of 6113 T cells that successfully provided the TCR VDJ sequence. MAIT cells have limited TCRα but diverse TCRβ repertoire. The TRBV expression was diverse but biased toward TRBV6-1, TRBV6-2, TRBV6-4 , and TRBV20-1 (Supplementary Material, Figure 2), similar to the previous report[46]. We also observed that all the recurrent GBM patients who were not treated with anti-PD1 therapy were positive for MAIT cells. Five of the nine newly diagnosed patients and three of the recurrent GBM patients with anti-PD1 treatment were positive for MAIT cells (Supplementary Table 5).

MAIT cells clustered with IL-17-producing T cells

We further analyzed the lymphoid cluster to delineate the lymphoid cell populations in GBM. Unsupervised clustering of the lymphoid cell population resulted in 13 subclusters (Figure 3C & Supplementary material, Figure 6), which included: one cytotoxic T cell cluster with expression of *GZMB*, *PRF1*, *GNLY*, and *KLRD1*; one central memory T cell cluster with expression of *IL7R*, *CD40LG*, *SELL*, *LEF1*, and *CCR7*; one exhausted T cell cluster with high *CD8A/B* and *TOX* expression; one resting NK cell cluster with high *ZBTB16* expression; one activated NK cell cluster with *XCL1* and *XCL2* expression; one Tregs cluster with *FOXP3* expression; one T cell cluster highly enriched in interferon stimulated genes (ISG) like *ISG15* and *ISG20*; one effector/memory T cell cluster which expressed markers of both effector T cells (expressing *GZMB*, *PRF1 & GNLY*) and memory T cells (*CCL5* & *IL7R*) (Supplementary material, Figure 4); one cluster high in the expression of cell proliferation marker (*MKI67*); one cluster highly enriched in genes that encode heat shock proteins like *HSPA1B;* and Th17-like T cell cluster with high expression of *RORC* and *KLRB1*; one MHC-II gene-enriched cluster with high expression

of *HLA-DQA1, HLA-DQB1, HLA_DQB2, HLA-DMA, HLA-DMB, HLA-DRA*; one antigen presenting cell (APC) cluster with high expression of MHC-II genes, *CD14*, *CD83, and CD68*. The heatmap showing the relative expression levels of the key marker genes of the lymphoid clusters is given in Figure 3D. The differentially expressed genes in the various lymphoid clusters are provided in Supplementary Table 6. These results showed the heterogeneity of T cell population within the GBM tumor. We also analyzed the distribution of the lymphoid cell population in MAIT-positive and MAIT-negative patient samples (Figure 3E). There was no significant difference in the distribution of the lymphoid subpopulations with respect to the MAIT negative/positive status of GBM patients.

Most of the MAIT cells identified from TCR sequencing were mapped to the Th17-like T cell cluster (Figure 3F). Cells in this cluster have a high expression of the transcription factor *RORC* that regulates *IL17* expression (Figure 3G). The cluster also showed high expression of the MAIT cell marker *CD161* (*KLRB1*) gene. Cells in this cluster also showed higher expression of *IL7R*, *CD40LG* and *IL2* when compared with the rest of the lymphoid cell clusters (Supplementary material, Figure 3). The high expression *RORC* indicated that these cells have the potential to produce IL-17. Differential gene expression analysis showed that the Th17-like T cell cluster has a higher expression of the *KLRB1*, *RORA*, *RORC*, *CCR6* and *CXCR6* which are genes expressed by IL-17-producing T cells[47]. The cells in the cluster showed low expression of the transcription factor gene *TBX21* as well as a low expression of the cytokine *IFNG*. The identification of MAIT cells with high *RORC* and low *TBX21* expressions suggested that MAIT cells in GBM tumors tissue skewed their function to secret IL-17.

Multiple pathways of TANs/MDSCs enriched in MAIT-positive patient samples

To further understand the transcriptomic differences between MAIT-positive and -negative samples defined with the bulk sequencing data analysis (Fig 2A), we conducted a GSEA with the bulk RNA-seq data from TCGA-GBM. Interestingly, the most significantly enriched process among all Gene Ontology Biological Process (GOBP)-processes, including non-immunological processes in MAIT-positive samples, was an immunological process, the negative regulation of immune response (GO:0050777, Figure 4A). Since the negative regulation of immune response is an integrated pathway including many immunosuppressive processes, this significant enrichment suggests that multiple immunosuppressive mechanisms are more active in MAIT-positive samples than in MAIT-negative samples. Multiple neutrophil migration/chemotaxis and neutrophil activation-related pathways were significantly enriched in MAIT-positive samples (Figure 4B). The enrichment of these gene sets in MAIT-positive samples went along with the finding that MAIT cells in GBM skewed their function to produce IL-17 since IL-17 induces chemotaxis and activation of neutrophils[23].

The biological characteristics of tumor-infiltrated neutrophils, called tumor-associated neutrophils (TANs), and blood-circulating neutrophils are significantly different[48]. Since we focused on tumor-derived transcriptomic data, all neutrophils in this study will be called TANs. Recently, it was reported that Neutrophil Degranulation (ND)-pathway genes were up-regulated in activated MDSCs[49]. Thus, the observed up-regulation of the ND-pathway can also be an indication of MDSC activation. Additionally, it is known that TANs and MDSCs share many morphological, functional, and transcriptomic characteristics and are difficult to distinguish from each other[50,51]. Therefore, the activities of TANs and MDSCs were evaluated simultaneously in the current study.

We next examined the TAN/MDSC activities in MAIT-positive/negative samples. GSEA, using the signature of Neutrophil Degranulation (NDsig) and of MDSC (MDSCsig), showed significant enrichment of those signatures in MAIT-positive samples (Figure 4C & 4D). These data indicated that TANs/MDSCs are highly activated in MAIT-positive samples compared with MAIT-negative samples.

TANs/MDSCs are known to suppress cancer immunity through various mechanisms[52,53]. The high *ARG1* expression by TANs/MDSCs depletes the local arginine[54], and the low arginine level impairs T cells by down-regulating CD3ζ chains[55]. TANs/MDSCs also express PD-L1 in cancer tumors which inhibits T cell functions[56]. The up-regulation of indoleamine 2,3-dioxygenase (IDO) depletes the local tryptophan and produces kynurenine, which inhibits T cell proliferation. The IL-10 and *TGF-β* produced by TANs/MDSCs suppress T cell proliferation/activity as well[57-59]. We examined the gene expressions of those molecules and found that all the genes were significantly up-regulated in MAIT-positive samples compared with MAIT-negative samples (Figure 5A). We observed the up-regulation of *ARG1* and the arginine reporter gene, *ASS1* (up-regulated upon the local arginine depletion), in MAIT-positive samples (Figure 5B & 5C). These data suggested that the multiple immunosuppressive pathways mediated by TANs/MDSCs were active in the MAIT-positive samples. Significantly negative correlations of TAN/MDSC activity with the overall survival indicated that their activities have an unfavorable impact on the GBM malignancy (Figure 5D).

Enrichment of genes for TANs/MDSCs in MAIT-positive patients aligns with our data showing that MAIT cells in GBM are MAIT17 since IL-17 is known to induce mechanisms to attract neutrophils. IL-17 triggers the production of CCL20 and G-CSF, which can act in synergy with other proinflammatory cytokines such as IL-6, IL-1α and IL-1β to recruit neutrophils[60].

MAIT-positive samples were higher in the expression of the genes *CCL20, IL1A, IL1B* and *IL6* in the TCGA-GBM data, suggesting that immunosuppressive myeloid cells could be recruited into the GBM tumor environment via an IL-17-dependent manner (Figure 5E). Altogether, these data strongly suggested that MAIT cells could induce the activation and recruitment of TANs/MDSCs through IL-17-mediated signaling, which exerts multiple immunosuppressive mechanisms in GBM.

To confirm the observation with a bulk RNAseq data set, TCGA-GBM, we analyzed myeloid cells from scRNA-seq data (Figure 3A). Unsupervised clustering of the myeloid cell population resulted in 13 clusters consisting of multiple microglia, macrophage, and one DC cell population (Figure 6A, 6B & Supplementary material, Figure 7). The myeloid clusters were characterized in the following ways: one inflammatory tumor-associated macrophages (TAMs) with high expression *IKZF1, and NFKB1* (Inflam-TAM); one *CCL3* high inflammatory TAM (CCL3-Inflam-TAM); Classical tumor-infiltrating monocytes (TIMs) with high *CD14* and *EGR1* expression (classical-TIM); two clusters of heat shock protein (HSP) enriched macrophages showed high expression for *HSPE1*, *HSPH1* and *HSPD1* (HSP-Macrophage1 and HSP-Macrophage2); one microglia enriched clusters with high *TMEM119* (Microglia); one cluster with high *VCAN, SERPINB2, CXCL2/3/5/8, S100A9* and *LYZ* expression (VCAN-TIM); DC cluster with high *LGALS2*, *FCER1A* and MHC II expression (DC); interferon-primed TAMs (IFN-TAM) with high *IFIT1/IFIT2, IFITM3*, and *ISG15*; proliferating cell cluster (Proliferating) with high *MKI67* expression; angio TAM with *GZMB, CXCR3, CXCR4* and *AREG* expression; One cluster of a mixture of myeloid and lymphoid cells with high *CD19* expression (Contaminant); one CD3-positive cluster with *CD3E*, *CD3D* expression within the myeloid population (CD3-positive). A cluster with mixed cell populations positive for myeloid cell markers or T-cell markers in a tumor

tissue has been reported in other study[28]. The differentially expressed genes in the myeloid cell clusters are provided in Supplementary Table 7. We could not find a significant difference in the distribution of the myeloid cell populations in MAIT-positive and MAIT-negative patients (Figure 6C).

Further clustering of the DC cell population resulted in 10 subclusters (Figure 6D & 6E). The DC clusters are characterized as follows: one activated mDC1 (migratory DC) with high expression of *CCR7, LAMP3, KYNU, IL7R* and *CLEC10A*; one migratory DC (mDC2) with high expression of *LAMP3, IL7* and *CCR7*; one cluster enriched in heat shock proteins (HSP-DC); one cluster with high mitochondrial gene expression (mito-DC); one cDC1 expressing *IRF8, BATF3, XCR1*; cDC2 with high *FCER1A* and *CD1C*. There were three monocyte-like DCs: mo-DC1 with high *CD14* and *C1QA* expression; Mo-DC2 expressing high *CD14, C1QA, CLEC9A* and Mo-DC3 with high expression of *CD14, C1QA, CCL3/4.* There was no significant difference in the distribution of the DC subpopulations between MAIT-positive and MAIT-negative groups. Differentially expressed genes in the DC clusters are given in Supplementary Table 8.

We also checked the expression of neutrophil marker genes *NAMPT*, *NEAT1*, *CD29*, *PAD14* and *LTF* in the scRNA-seq data however, we could not find clusters with expression of neutrophil markers. Neutrophils are known to have a low transcriptomic content, expressing only 300 to 350 genes and have a short life span, which results in low representation in sequencing[61-63]. We have also tried implementing the recommended protocol to improve neutrophil capturing by including low-UMI barcodes, however, we could not detect neutrophils.

Pan-cancer analysis showed a significant correlation between MAIT cell signature gene expression level and poor prognosis in two cancer types

The results obtained by the TCGA-GBM dataset strongly suggested the existence of a novel MAIT-TAN/MDSC pathway that potentially suppresses tumor immune responses. We next asked if the correlations found in GBM could also be found in other types of cancer. In the current study, we could not access enough FASTQ data files to examine the MAIT cell infiltration in different cancer types. Thus, we focused on investigating the relationship between the expression level of MAIT cell signature genes (*SLC4A10*, *MAF* and *CXCR4*) and the prognosis of 33 cancer types in the TCGA database (Supplementary Table 9). The samples in the dataset were bifurcated into MAIT-high or MAIT-low groups based on the expression value of the MAIT signature genes. In colon adenocarcinoma (COAD) and stomach adenocarcinoma (STAD), high expression of MAIT signature genes correlated with poor survival (Figure 7A). We then asked if TANs/MDSCs are involved in the MAIT cell-involving mechanism that significantly correlates with the disease prognosis. We performed GSEA using the NDsig and MDSCsig gene sets (Supplementary Table 3) and found that COAD and STAD showed a strong trend in up-regulation of both NDsig and MDSCsig in the MAIT-high group (Figure 7B). We also validated this observation by using the GOBP signature, and all neutrophil-related pathways significantly enriched in each MAIT-high group were extracted. COAD and STAD, which had significant up-regulation of TAN/MDSC activities, showed significant up-regulation of multiple neutrophil-related pathways in the MAIT-high group (Figure 7C). These results suggested that the MAIT-TAN/MDSC pathway is also active in COAD and STAD.

Discussion

In the current study, we identified MAIT cells in the GBM tissue by a single-cell TCR VDJ sequencing and found that more than half of GBM patient tumor tissues contained MAIT cells.

The immunological role of MAIT cells in cancer is unsettled given that MAIT cells either promote or suppress tumor growth varies depending on the cancer type. In the context of GBM, a limited number of studies on MAIT cells have been conducted. Peterfalvi et al., detected MAIT TCR transcripts in GBM samples[64]. Priya and Brutkiewicz demonstrated that MAIT cells could lyse GBM cells in vitro when the cells present riboflavin, 5-OP-RU[65]. To our knowledge, this is the first study demonstrating the existence of MAIT cells in GBM tissue relevant to the disease prognosis.

MAIT cells are classified into RORγ-t-expressing MAIT17 cells and T-bet-expressing MAIT1 cells that secrete IL-17 and IFN-γ upon stimulation[66]. The distribution of these functionally distinct MAIT cell subtypes varies across different tissues[67] Interestingly, most MAIT cells in GBM tissue expressed *RORC* (encoding RORγ-t), indicating that they were MAIT17 (Figure 3G). Corroborating with the data from scRNA-seq, we also found with TCGA-GBM data analysis that the expression levels of *IL17A* and *TNF* were significantly higher in MAIT-positive samples, while there was no statistical difference in *IFNG* expression between MAIT-positive and MAIT-negative samples. The skewing of MAIT function toward IL-17 production in cancer has been reported in other studies. Yan et al, (2020) reported that tumor-infiltrating MAIT cells enhanced the production of IL-17 and TNF-γ while the IFN-γ production level was not changed[19]. In colon adenocarcinomas, MAIT cells showed reduced IFN-γ production[68]. In hepatocellular carcinoma (HCC), dysfunctional MAIT cells were reported with altered transcriptional factor profiles, switching MAIT cells from a Th1-like to Th17-like phenotype with increased RORγ-t expression and a significantly reduced T-bet expression[18]. In multiple melanoma (MM), decreased MAIT percentage in PBMC compared with healthy control and a decrease in effector functional capacity of circulating MAIT cells, characterized by reduction of IFN-γ production was reported[15]. The

skewing mechanism of the MAIT cells is not well understood; however, the decrease in IFN-γ expression and increased IL-17 could have various implications for cancer. An effective mechanism for cancer to evade immune response is the dysfunction of the effector T-cells[69]. Tumor cells can employ various mechanisms to suppress IFN-γ signaling and render T cells ineffective[70]. In murine models, MAIT cell dysfunction characterized by high expression of PD-1 and TIM-3 was reported[18]. These MAIT cells showed significantly lower expression of IFN-γ. Over time, the increase in the dysfunction of MAIT cells was accompanied by loss of IFN-γ production. Therefore, the decrease in the IFN-γ expression in MAIT cells in GBM could be a sign of the dysfunction of these cells. IL-17 is a cytokine associated with the development and pro-tumor function of immuno-suppressive myeloid cells[71-73]. Taken together, the skewing of MAIT cell function could be an effective mechanism to dysregulate the MAIT cell function and promote immune suppression in GBM. Along with this line, we also found that the expression levels of MAIT signature genes correlated with poor disease outcomes of GBM patients in multiple patient data sets (Figure 1I - 1N), suggesting that MAIT cells in GBM may contribute to immune suppression in the patients.

We found that the frequency of MAIT cells among T cells in GBM tissues that contain MAIT cells was 1.46%. In contrast, the frequency of MAIT cells among T cells in peripheral blood samples of GBM patients was 0.45% (median frequency of 8 patients), which was significantly lower than that of healthy donors. Although the GBM tissue samples and peripheral blood samples were from different sets of GBM patients, this observation strongly suggested the enrichment of MAIT cells in GBM tissues. Similar to our observation made in this study, the significant reduction of MAIT cells in the circulation in cancer patients has been reported in other types of cancer including colorectal, lung and liver[20,74,75]. In colorectal cancer, a decrease in circulating

MAIT cells was associated with increased infiltrated MAIT cells[21,75]. More interestingly, the frequency of MAIT cells in cancer tissues correlated with the advancement of the disease in colorectal cancer patients[75]. Together with our observation on the negative correlations between MAIT signature gene expression levels and patient survival in TCGA-GBM and CGGA data sets, MAIT cells in cancer tissues may contribute to the formation of immunosuppressive tumor microenvironment in certain types of cancer.

The level of TAN infiltration has been reported to correlate with the grades of glioma, and some tumor-promoting mechanisms by TANs in GBM have been suggested[76,77]. However, the mechanisms attracting TANs to the GBM tissue and their activation mechanism are not well understood. Our study observed a significant correlation between the expression level of MAIT cell signature genes and the activation level of TANs/MDSCs. MAIT cells rapidly secrete a large amount of cytokines, including IL-17[10], which is important in this context as IL-17 promotes the local attraction and activation of TANs through the induction of chemokines[13,14]. We observed that MAIT cells express *RORC* by scRNA-seq and a significant up-regulation of *IL17A* in MAIT-positive samples in TCGA-GBM data. Concurrently, the activation of TANs/MDSCs and multiple neutrophil attraction pathways were up-regulated in MAIT-positive samples. These observations suggested the contribution of MAIT cells to recruit TANs in GBM tissues.

Neutrophils can exert strong cytotoxicity; therefore, they may play anti-tumor roles. However, the biological function of neutrophils can be modified by the tissue environment, especially by the local TGF-β status. Under a TGF-β depleted environment, neutrophils tend to acquire the anti-tumor phenotype, called N1, whereas, under the TGF-β sufficient environment, they tend to acquire the pro-tumor phenotype, called N2[53]. The immunosuppressive and tumor-promoting role of N2-TAN has been reported in multiple cancer types. Since the expression level of *TGFB1* in

MAIT-positive samples was significantly up-regulated (Figure 5A), the TME of MAIT-positive patients is the preferred environment for TANs to acquire N2 phenotype. Thus, the TANs in MAIT-positive GBM samples are considered to play a relatively immunosuppressive role and can cause GBM's poor prognosis.

MDSCs suppress cancer immunity[52]. In GBM, their immunosuppressive role and the correlation between their infiltration and poor survival were reported[78]. He, et al. showed that MDSCs have phenotypic plasticity in their immunosuppressive function using *in vivo* cancer model and IL-17 was required for the development of MDSCs in tumor-bearing mice and for exerting MDSC's pro-tumor functions[73]. Guan, et al. also observed a significant correlation between the tumor IL-17 level and the MDSC infiltration level in renal cancer[79]. These reports support our hypothesis that the IL-17 secreted from MAIT cells can attract MDSCs and promote their immunosuppressive function in GBM.

Although we found MAIT cells in GBM tissues from patients, it is not clear how they get activated in the cancer tissue to express their functions. MAIT cells recognize bacteria metabolites, riboflavin. Recently, Naghavian et al. reported that bacteria-specific peptide antigens were presented in GBM tissues[80]. This study may raise the possibility that MAIT cells in GBM could be activated by bacteria metabolites that could reach the brain. Antigens recognized by MAIT cells are not fully understood. A study by Zhang et al., reporting the role of MAIT cells residing in the meninges contributing to the formation of memory by producing antioxidant molecules, suggested that MAIT cells get activated by recognizing unknown antigens existing in the brain[81]. MAIT cells in GBM may recognize the same antigen to express their function.

In conclusion, we propose a novel MAIT-TAN/MDSC pathway that could contribute to the poor prognosis of GBM (Figure 8). MAIT cells could be a missing link between GBM and

TAN/MDSC's activation and infiltration. The current study sheds light on the possible immunosuppressive role of MAIT cells in GBM.

Acknowledgement:

The results published here are in part based upon data generated by the TCGA Research Network: https://www.cancer.ov/tcga.

Authorship Statement:

Conceptualization: S.K., T.H, M.T.; Investigation: S.K., T.H., M.T., A.L., R.P., H.K, M.C, A.H, M. Watowitch, M. Watanabe, M.G; Writing: S.K, T.H, M.T., H.K., A.L.; Funding acquisition: M.T., R.P., M.R.G. All authors read and approved the manuscript.

References

1. Roy S, Lahiri D, Maji T, Biswas J. Recurrent glioblastoma: where we stand. *South Asian journal of cancer.* 2015; 4(4):163.
2. Balana C, Vaz MA, Manuel Sepúlveda J, et al. A phase II randomized, multicenter, open-label trial of continuing adjuvant temozolomide beyond 6 cycles in patients with glioblastoma (GEINO 14-01). *Neuro-oncology.* 2020; 22(12):1851-1861.
3. Stupp R, Taillibert S, Kanner A, et al. Effect of tumor-treating fields plus maintenance temozolomide vs maintenance temozolomide alone on survival in patients with glioblastoma: a randomized clinical trial. *Jama.* 2017; 318(23):2306-2316.
4. Omuro A, Vlahovic G, Lim M, et al. Nivolumab with or without ipilimumab in patients with recurrent glioblastoma: results from exploratory phase I cohorts of CheckMate 143. *Neuro-oncology.* 2018; 20(5):674-686.
5. Klemm F, Maas RR, Bowman RL, et al. Interrogation of the microenvironmental landscape in brain tumors reveals disease-specific alterations of immune cells. *Cell.* 2020; 181(7):1643-1660. e1617.
6. Kubica P, Lara-Velazquez M, Bam M, et al. MR1 overexpression correlates with poor clinical prognosis in glioma patients. *Neuro-Oncology Advances.* 2021; 3(1):vdab034.
7. Crowther MD, Dolton G, Legut M, et al. Genome-wide CRISPR–Cas9 screening reveals ubiquitous T cell cancer targeting via the monomorphic MHC class I-related protein MR1. *Nature immunology.* 2020; 21(2):178-185.
8. Vacchini A, Chancellor A, Yang Q, et al. Nucleobase adducts bind MR1 and stimulate MR1-restricted T cells. *Science Immunology.* 2024; 9(95):eadn0126.
9. Cogswell DT, Gapin L, Tobin HM, McCarter MD, Tobin RP. MAIT cells: partners or enemies in cancer immunotherapy? *Cancers.* 2021; 13(7):1502.
10. Dusseaux M, Martin E, Serriari N, et al. Human MAIT cells are xenobiotic-resistant, tissue-targeted, CD161hi IL-17–secreting T cells. *Blood, The Journal of the American Society of Hematology.* 2011; 117(4):1250-1259.
11. Lezmi G, Abou-Taam R, Garcelon N, et al. Evidence for a MAIT-17–high phenotype in children with severe asthma. *Journal of Allergy and Clinical Immunology.* 2019; 144(6):1714-1716. e1716.

12. Lu B, Liu M, Wang J, et al. IL-17 production by tissue-resident MAIT cells is locally induced in children with pneumonia. *Mucosal Immunology.* 2020; 13(5):824-835.

13. Parajuli P, Mittal S. Role of IL-17 in glioma progression. *Journal of spine & neurosurgery.* 2013.

14. Wu L, Awaji M, Saxena S, Varney ML, Sharma B, Singh RK. IL-17–CXC chemokine receptor 2 axis facilitates breast cancer progression by up-regulating neutrophil recruitment. *The American journal of pathology.* 2020; 190(1):222-233.

15. Gherardin NA, Loh L, Admojo L, et al. Enumeration, functional responses and cytotoxic capacity of MAIT cells in newly diagnosed and relapsed multiple myeloma. *Scientific reports.* 2018; 8(1):4159.

16. Priya R, Brutkiewicz RR. MR1 Tetramer–Based Artificial APCs Expand MAIT Cells from Human Peripheral Blood That Effectively Kill Glioblastoma Cells. *Immunohorizons.* 2021; 5(6):500-511.

17. Ruf B, Catania VV, Wabitsch S, et al. Activating mucosal-associated invariant T cells induces a broad antitumor response. *Cancer immunology research.* 2021; 9(9):1024-1034.

18. Ruf B, Bruhns M, Babaei S, et al. Tumor-associated macrophages trigger MAIT cell dysfunction at the HCC invasive margin. *Cell.* 2023; 186(17):3686-3705. e3632.

19. Yan J, Allen S, McDonald E, et al. MAIT cells promote tumor initiation, growth, and metastases via tumor MR1. *Cancer discovery.* 2020; 10(1):124-141.

20. Duan M, Goswami S, Shi J-Y, et al. Activated and exhausted MAIT cells foster disease progression and indicate poor outcome in hepatocellular carcinoma. *Clinical Cancer Research.* 2019; 25(11):3304-3316.

21. Zabijak L, Attencourt C, Guignant C, et al. Increased tumor infiltration by mucosal-associated invariant T cells correlates with poor survival in colorectal cancer patients. *Cancer immunology, immunotherapy.* 2015; 64:1601-1608.

22. Peterfalvi A, Gomori E, Magyarlaki T, et al. Invariant Vα7. 2-Jα33 TCR is expressed in human kidney and brain tumors indicating infiltration by mucosal-associated invariant T (MAIT) cells. *International immunology.* 2008; 20(12):1517-1525.

23. Ge Y, Huang M, Yao Y-m. Biology of interleukin-17 and its pathophysiological significance in sepsis. *Frontiers in immunology.* 2020; 11:548387.

24. Louis DN, Perry A, Wesseling P, et al. The 2021 WHO classification of tumors of the central nervous system: a summary. *Neuro-oncology.* 2021; 23(8):1231-1251.

25. Cloughesy TF, Mochizuki AY, Orpilla JR, et al. Neoadjuvant anti-PD-1 immunotherapy promotes a survival benefit with intratumoral and systemic immune responses in recurrent glioblastoma. *Nature Medicine.* 2019; 25(3):477-+.

26. Hao Y, Stuart T, Kowalski MH, et al. Dictionary learning for integrative, multimodal and scalable single-cell analysis. *Nature biotechnology.* 2024; 42(2):293-304.

27. Ma RY, Black A, Qian BZ. Macrophage diversity in cancer revisited in the era of single-cell omics. *Trends in Immunology.* 2022; 43(7):546-563.

28. Lee AH, Sun L, Mochizuki AY, et al. Neoadjuvant PD-1 blockade induces T cell and cDC1 activation but fails to overcome the immunosuppressive tumor associated macrophages in recurrent glioblastoma. *Nat Commun.* 2021; 12(1):6938.

29. Law CW, Alhamdoosh M, Su S, et al. RNA-seq analysis is easy as 1-2-3 with limma, Glimma and edgeR. *F1000Research.* 2016; 5.

30. Abdelfattah N, Kumar P, Wang C, et al. Single-cell analysis of human glioma and immune cells identifies S100A4 as an immunotherapy target. *Nat Commun.* 2022; 13(1):767.

31. Budczies J, Klauschen F, Sinn BV, et al. Cutoff Finder: a comprehensive and straightforward Web application enabling rapid biomarker cutoff optimization. *PloS one.* 2012; 7(12):e51862.

32. Uhlen M, Zhang C, Lee S, et al. A pathology atlas of the human cancer transcriptome. *Science.* 2017; 357(6352):eaan2507.

33. Zhao Z, Zhang K-N, Wang Q, et al. Chinese Glioma Genome Atlas (CGGA): a comprehensive resource with functional genomic data from Chinese glioma patients. *Genomics, Proteomics and Bioinformatics.* 2021; 19(1):1-12.

34. Alshetaiwi H, Pervolarakis N, McIntyre LL, et al. Defining the emergence of myeloid-derived suppressor cells in breast cancer using single-cell transcriptomics. *Science immunology.* 2020; 5(44):eaay6017.

35. Pesenacker AM, Wang AY, Singh A, et al. A regulatory T-cell gene signature is a specific and sensitive biomarker to identify children with new-onset type 1 diabetes. *Diabetes.* 2016; 65(4):1031-1039.

36. Cancer Genome Atlas Research N. Comprehensive genomic characterization defines human glioblastoma genes and core pathways. *Nature.* 2008; 455(7216):1061-1068.

37. Zhang K, Liu X, Li G, et al. Clinical management and survival outcomes of patients with different molecular subtypes of diffuse gliomas in China (2011–2017): a multicenter retrospective study from CGGA. *Cancer biology & medicine.* 2022; 19(10):1460.

38. Zhao Z, Meng F, Wang W, Wang Z, Zhang C, Jiang T. Comprehensive RNA-seq transcriptomic profiling in the malignant progression of gliomas. *Scientific data.* 2017; 4(1):1-7.

39. Howson LJ, Awad W, von Borstel A, et al. Absence of mucosal-associated invariant T cells in a person with a homozygous point mutation in MR1. *Science immunology.* 2020; 5(49):eabc9492.

40. Flavahan WA, Drier Y, Liau BB, et al. Insulator dysfunction and oncogene activation in IDH mutant gliomas. *Nature.* 2016; 529(7584):110-114.

41. Darmanis S, Sloan SA, Croote D, et al. Single-cell RNA-seq analysis of infiltrating neoplastic cells at the migrating front of human glioblastoma. *Cell reports.* 2017; 21(5):1399-1410.

42. De Biasi S, Gibellini L, Lo Tartaro D, et al. Circulating mucosal-associated invariant T cells identify patients responding to anti-PD-1 therapy. *Nature communications.* 2021; 12(1):1669.

43. Guo X, Zhang Y, Zheng L, et al. Global characterization of T cells in non-small-cell lung cancer by single-cell sequencing. *Nature medicine.* 2018; 24(7):978-985.

44. Park D, Kim HG, Kim M, et al. Differences in the molecular signatures of mucosal-associated invariant T cells and conventional T cells. *Scientific Reports.* 2019; 9(1):7094.

45. Brennan CW, Verhaak RG, McKenna A, et al. The somatic genomic landscape of glioblastoma. *cell.* 2013; 155(2):462-477.

46. Garner LC, Amini A, FitzPatrick ME, et al. Single-cell analysis of human MAIT cell transcriptional, functional and clonal diversity. *Nature Immunology.* 2023; 24(9):1565-1578.

47. Gray EH, Srenathan U, Durham LE, et al. Phenotypic, molecular and functional characterisation of human in vitro-generated IL-17A+ CD8+ T-cells. *bioRxiv.* 2022:2022.2011. 2014.516164.

48. Mollinedo F. Neutrophil degranulation, plasticity, and cancer metastasis. *Trends in immunology.* 2019; 40(3):228-242.

49. Dean MJ, Ochoa JB, Sanchez-Pino MD, et al. Severe COVID-19 is characterized by an impaired type I interferon response and elevated levels of arginase producing granulocytic myeloid derived suppressor cells. *Frontiers in immunology.* 2021; 12:695972.

50. Zhou J, Nefedova Y, Lei A, Gabrilovich D. Neutrophils and PMN-MDSC: Their biological role and interaction with stromal cells. Paper presented at: Seminars in immunology2018.

51. Aarts CE, Kuijpers TW. Neutrophils as myeloid-derived suppressor cells. *European journal of clinical investigation.* 2018; 48:e12989.

52. Yang Y, Li C, Liu T, Dai X, Bazhin AV. Myeloid-derived suppressor cells in tumors: from mechanisms to antigen specificity and microenvironmental regulation. *Frontiers in immunology.* 2020; 11:540749.

53. Masucci MT, Minopoli M, Carriero MV. Tumor associated neutrophils. Their role in tumorigenesis, metastasis, prognosis and therapy. *Frontiers in oncology.* 2019; 9:1146.

54. Grzywa TM, Sosnowska A, Matryba P, et al. Myeloid cell-derived arginase in cancer immune response. *Frontiers in immunology.* 2020; 11:536322.

55. Rodriguez PC, Zea AH, DeSalvo J, et al. l-arginine consumption by macrophages modulates the expression of CD3ζ chain in T lymphocytes. *The Journal of Immunology.* 2003; 171(3):1232-1239.

56. Ballbach M, Dannert A, Singh A, et al. Expression of checkpoint molecules on myeloid-derived suppressor cells. *Immunology Letters.* 2017; 192:1-6.

57. Li F, Zhao Y, Wei L, Li S, Liu J. Tumor-infiltrating Treg, MDSC, and IDO expression associated with outcomes of neoadjuvant chemotherapy of breast cancer. *Cancer biology & therapy.* 2018; 19(8):695-705.

58. Taga K, Tosato G. IL-10 inhibits human T cell proliferation and IL-2 production. *Journal of immunology (Baltimore, Md.: 1950).* 1992; 148(4):1143-1148.

59. Dahmani A, Delisle J-S. TGF-β in T cell biology: implications for cancer immunotherapy. *Cancers.* 2018; 10(6):194.

60. Ge Y, Huang M, Yao YM. Biology of Interleukin-17 and Its Pathophysiological Significance in Sepsis. *Front Immunol.* 2020; 11:1558.

61. Hay SB, Ferchen K, Chetal K, Grimes HL, Salomonis N. The Human Cell Atlas bone marrow single-cell interactive web portal. *Experimental hematology.* 2018; 68:51-61.

62. Dancey J, Deubelbeiss KA, Harker LA, Finch CA. Neutrophil kinetics in man. *The Journal of clinical investigation.* 1976; 58(3):705-715.

63. Summers C, Rankin SM, Condliffe AM, Singh N, Peters AM, Chilvers ER. Neutrophil kinetics in health and disease. *Trends in immunology.* 2010; 31(8):318-324.

64. Peterfalvi A, Gomori E, Magyarlaki T, et al. Invariant Valpha7.2-Jalpha33 TCR is expressed in human kidney and brain tumors indicating infiltration by mucosal-associated invariant T (MAIT) cells. *Int Immunol.* 2008; 20(12):1517-1525.

65. Priya R, Brutkiewicz RR. MR1 Tetramer-Based Artificial APCs Expand MAIT Cells from Human Peripheral Blood That Effectively Kill Glioblastoma Cells. *Immunohorizons.* 2021; 5(6):500-511.

66. Cogswell DT, Gapin L, Tobin HM, McCarter MD, Tobin RP. MAIT Cells: Partners or Enemies in Cancer Immunotherapy? *Cancers (Basel).* 2021; 13(7).

67. Pellicci DG, Koay H-F, Berzins SP. Thymic development of unconventional T cells: how NKT cells, MAIT cells and γδ T cells emerge. *Nature Reviews Immunology.* 2020; 20(12):756-770.

68. Sundström P, Ahlmanner F, Akéus P, et al. Human mucosa-associated invariant T cells accumulate in colon adenocarcinomas but produce reduced amounts of IFN-γ. *The Journal of Immunology.* 2015; 195(7):3472-3481.

69. Chiou S-H, Sheu B-C, Chang W-C, Huang S-C, Hong-Nerng H. Current concepts of tumor-infiltrating lymphocytes in human malignancies. *Journal of reproductive immunology.* 2005; 67(1-2):35-50.

70. Han J, Wu M, Liu Z. Dysregulation in IFN-γ signaling and response: the barricade to tumor immunotherapy. *Frontiers in Immunology.* 2023; 14:1190333.

71. Yang Y, Li C, Liu T, Dai X, Bazhin AV. Myeloid-Derived Suppressor Cells in Tumors: From Mechanisms to Antigen Specificity and Microenvironmental Regulation. *Front Immunol.* 2020; 11:1371.

72. De Leo A, Ugolini A, Veglia F. Myeloid Cells in Glioblastoma Microenvironment. *Cells.* 2020; 10(1).

73. He D, Li H, Yusuf N, et al. IL-17 promotes tumor development through the induction of tumor promoting microenvironments at tumor sites and myeloid-derived suppressor cells. *The Journal of Immunology.* 2010; 184(5):2281-2288.

74. Shi L, Lu J, Zhong D, et al. Clinicopathological and predictive value of MAIT cells in non-small cell lung cancer for immunotherapy. *Journal for immunotherapy of cancer.* 2023; 11(1).

75. Ling L, Lin Y, Zheng W, et al. Circulating and tumor-infiltrating mucosal associated invariant T (MAIT) cells in colorectal cancer patients. *Sci Rep.* 2016; 6:20358.

76. Liang J, Piao Y, Holmes L, et al. Neutrophils promote the malignant glioma phenotype through S100A4. *Clin Cancer Res.* 2014; 20(1):187-198.

77. Fossati G, Ricevuti G, Edwards SW, Walker C, Dalton A, Rossi ML. Neutrophil infiltration into human gliomas. *Acta Neuropathol.* 1999; 98(4):349-354.

78. De Leo A, Ugolini A, Veglia F. Myeloid cells in glioblastoma microenvironment. *Cells.* 2020; 10(1):18.

79. Guan X, Liu Z, Zhang J, Jin X. Myeloid-derived suppressor cell accumulation in renal cell carcinoma is correlated with CCL2, IL-17 and IL-18 expression in blood and tumors. *Advances in Clinical and Experimental Medicine.* 2018; 27(7):947-953.

80. Naghavian R, Faigle W, Oldrati P, et al. Microbial peptides activate tumour-infiltrating lymphocytes in glioblastoma. *Nature.* 2023; 617(7962):807-817.

81. Zhang Y, Bailey JT, Xu E, et al. Mucosal-associated invariant T cells restrict reactive oxidative damage and preserve meningeal barrier integrity and cognitive function. *Nat Immunol.* 2022; 23(12):1714-1725.

Figure Legends

Figure 1. **MAIT cell in PBMC and evaluation of clinical prognosis (A)** MAIT cells of total T cells in PBMC of GBM patients compared with healthy control. **(B)** Percentage of MAIT cells secreting IFN-γ, IL17 or TNF-α **(C)** Expression of MR1 **(D &E)** The correlation between MR1 expression and GBM survival **(F)** The mutational schema in MR1 locus **(G)** H3K27ac ChIP peaks in MR1 locus of GBM (GBM2w, IDHwt) and high-grade glioma (AA15m, IDHmut) samples. **(H)** tSNE plots of single-cell RNA-seq data from GBM tissues of four patients. Colored dots represent MR1-expressing cells. The correlation between expression of MAIT cell markers SLC4A10 **(I)** CXCR4 **(J)** and MAF **(K)** and GBM survival in TCGA-GBM. The correlation between expression of MAIT cell markers SLC4A10 **(L)** CXCR4 **(M)** and MAF **(N)** and GBM patients survival in CGGA.

Figure 2. Multi-faceted evaluation of the MAIT infiltrated samples in TCGA-GBM. Multi-faceted evaluation of the MAIT infiltrated samples in TCGA-GBM. **(A)** The levels of MAIT cell infiltration in TCGA-GBM samples. **(B** & **C)** Gene expression levels of MAIT cell surface receptors/secreting cytokines. **(D)** Color map showing multiple clinical/molecular indicators. Molecular indicators' information was obtained from a previously reported database, and the neural samples were integrated into the proneural samples. **(E)** The distribution of GBM subtypes among samples **(F)** MR1 expression in MAIT positive and –negative patient samples.

Figure 3. Single-cell RNA sequencing data analysis of GBM patient samples and identification of MAIT cells. Unsupervised clustering of the CD45+ cells from 23 samples showed 3 clusters. (A) UMAP of CD45+ cells (B) Heat map of MAIT cell counts identified per

sample from TCR sequencing (C) UMAP of lymphoid cell population from GBM scRNA-seq data (D) Heat map of marker genes for lymphoid cells clusters (E) Distribution of lymphoid cell populations across samples (F) MIAT cells (Black) identified from TCR sequencing projected on UMAP. Th17-like T cells are shown in orange color (G) *RORC* gene expression projected on UMAP.

Figure 4. Evaluations of the activity of TANs/MDSCs in MAIT-positive/negative samples. GSEA Enrichment score of pathways **(A)** Negative regulation of immune response **(B)** Neutrophil related genes enriched in MAIT-positive samples **(C)** Neutrophil Degranulation **(D)** MDSC signature

Figure 5. Evaluations of the activity of TANs/MDSCs in MAIT-positive/negative samples. **(A)** Differential expression levels of the immunosuppressive pathway genes related to TANs/MDSCs. Violin plots of **(B & C)** ARG1 & ASS1 in MAIT-positive/negative samples. **(D)** Prognostic correlations of NDsig-index and MDSCsig-index with TCGA-GBM clinical data. Cut off: NDsig-index = 41.89, MDSCsig-index = 27.48. **(E)** Expression of CCL20, IL1A, IL1B and IL6 involved in IL17 mediated TAN/MDSC recruitment upregulated in MAIT positive patients.

Figure 6. Analysis of myeloid cell populations (A) UMAP of myeloid cell population **(B)** Heatmap of markers for the myeloid clusters **(C)** Distribution of cell types between MAIT-Positive and MAIT-Negative samples **(D)** UMAP of Dendritic cell populations in GBM patient samples **(E)** Heatmap of the markers for the different DC clusters. The cluster annotation in the DC population in **(D)** and **(E)** are as follows: Two migratory DC (mDC1 & mDC2), DC cluster

with high expression of heat shock proteins (HSP-DC), DC cluster with high expression of mitochondrial genes (mito-DC), two cDC clusters (cDC1 & cDC2) and three monocytic DC clusters (mo-DC1 & mo-DC2).

Figure 7. **Correlations between MAIT cell signature genes, prognosis, and TANs/MDSCs in pan-cancer analyses**. **(A)** The prognostic correlations of MAIT cell signature genes in colon adenocarcinoma (COAD) and stomach adenocarcinoma (STAD). **(B)** GSEA plots for multiple COAD and STAD. MAIT signature genes-high/low groups were compared. **(C)** GSEA results of neutrophil related pathways in the MAIT signature genes-high group. All pathways shown were significant ($q < 0.05$).

Figure 1.

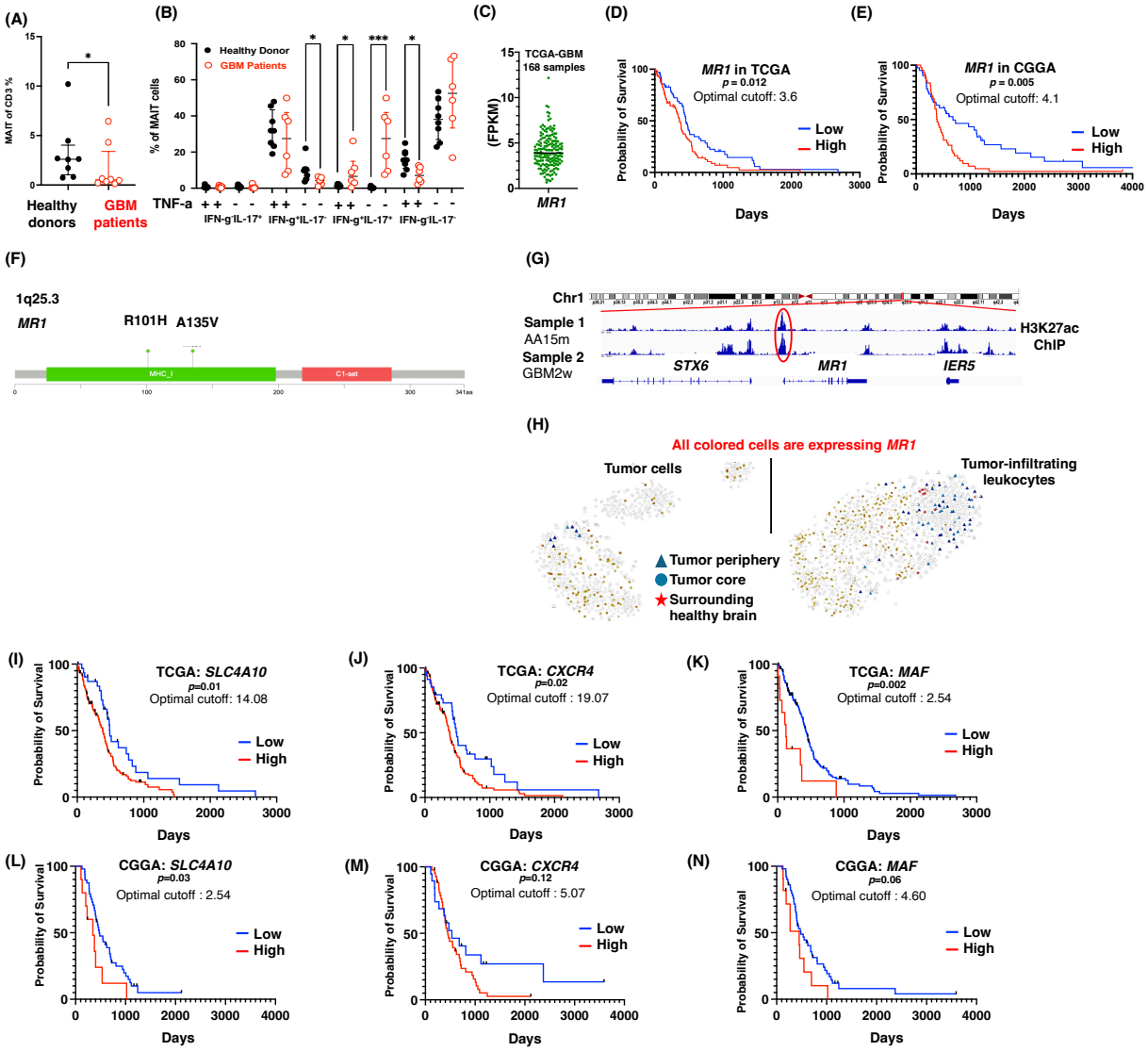
(A)
MAIT of CD3 %
Healthy donors
GBM patients
(B)
Healthy Donor
GBM Patients
% of MAIT cells
TNF-a
IFN-g+IL-17+
IFN-g+IL-17-
IFN-g-IL-17+
IFN-g-IL-17-
(C)
TCGA-GBM
168 samples
(FPKM)
MR1
(D)
MR1 in TCGA
p = 0.012
Optimal cutoff: 3.6
Low
High
Probability of Survival
Days
(E)
MR1 in CGGA
p = 0.005
Optimal cutoff: 4.1
(F)
1q25.3
MR1
R101H
A135V
MHC_I
C1-set
(G)
Chr1
Sample 1
AA15m
Sample 2
GBM2w
H3K27ac
ChIP
STX6
MR1
IER5
(H)
All colored cells are expressing MR1
Tumor cells
Tumor-infiltrating leukocytes
Tumor periphery
Tumor core
Surrounding healthy brain
(I)
TCGA: SLC4A10
p=0.01
Optimal cutoff: 14.08
(J)
TCGA: CXCR4
p=0.02
Optimal cutoff : 19.07
(K)
TCGA: MAF
p=0.002
Optimal cutoff : 2.54
(L)
CGGA: SLC4A10
p=0.03
Optimal cutoff : 2.54
(M)
CGGA: CXCR4
p=0.12
Optimal cutoff : 5.07
(N)
CGGA: MAF
p=0.06
Optimal cutoff : 4.60

Figure 2.

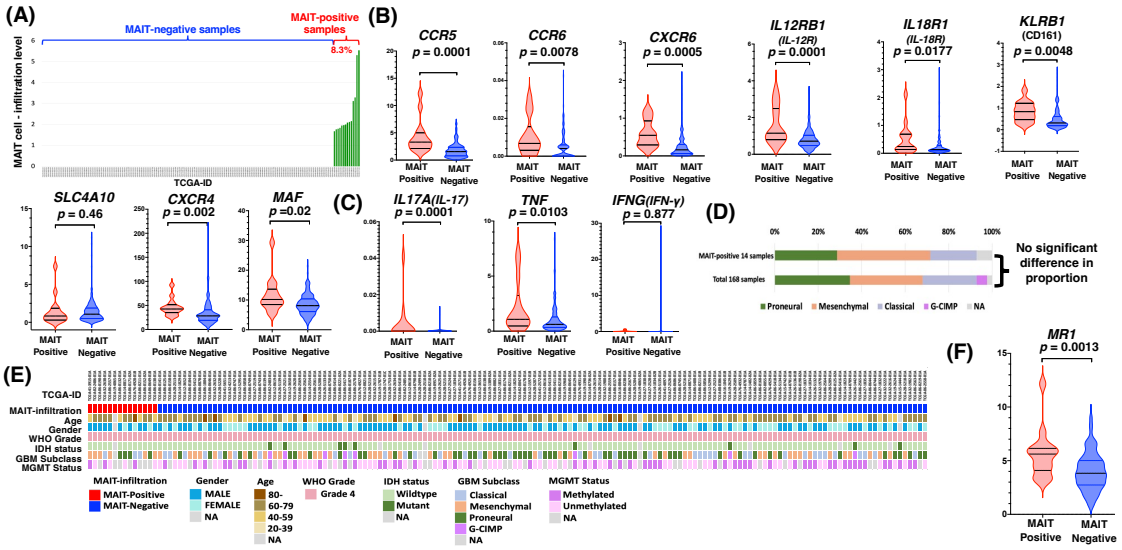
(A)
MAIT-negative samples
MAIT-positive samples
8.3%
MAIT cell - infiltration level
TCGA-ID
(B)
CCR5 p = 0.0001
CCR6 p = 0.0078
CXCR6 p = 0.0005
IL12RB1 (IL-12R) p = 0.0001
IL18R1 (IL-18R) p = 0.0177
KLRB1 (CD161) p = 0.0048
SLC4A10 p = 0.46
CXCR4 p = 0.002
MAF p =0.02
(C)
IL17A(IL-17) p = 0.0001
TNF p = 0.0103
IFNG(IFN-γ) p = 0.877
MAIT Positive
MAIT Negative
(D)
MAIT-positive 14 samples
Total 168 samples
No significant difference in proportion
Proneural
Mesenchymal
Classical
G-CIMP
NA
(E)
TCGA-ID
MAIT-infiltration
Age
Gender
WHO Grade
IDH status
GBM Subclass
MGMT Status
MAIT-Positive
MAIT-Negative
MALE
FEMALE
80-
60-79
40-59
20-39
Grade 4
Wildtype
Mutant
Classical
Mesenchymal
Proneural
G-CIMP
Methylated
Unmethylated
(F)
MR1 p = 0.0013

Figure 3.

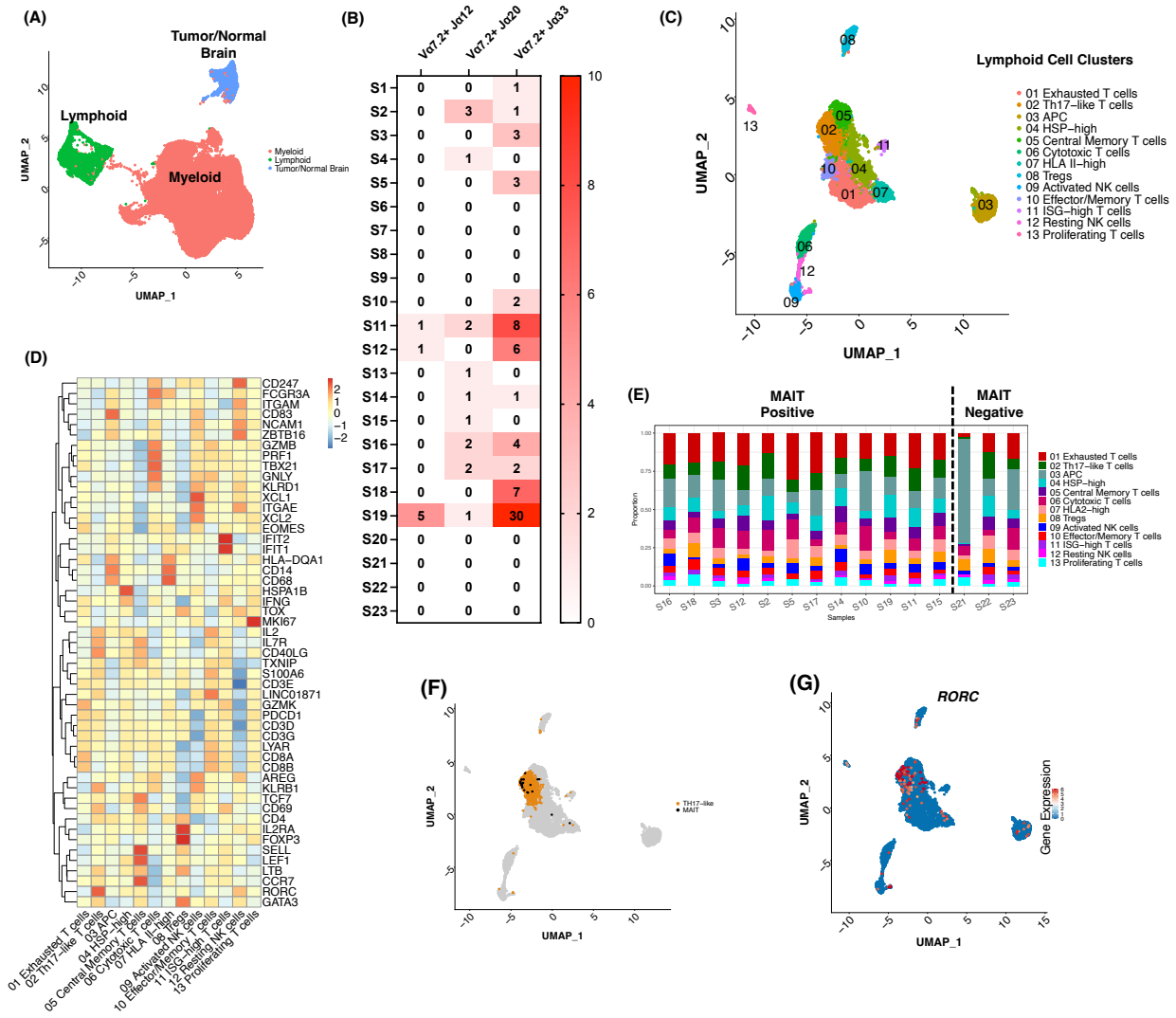
(A)
Tumor/Normal Brain
Lymphoid
Myeloid
Myeloid
Lymphoid
Tumor/Normal Brain
UMAP_2
UMAP_1
(B)
Vd7.2+ Jd12
Vd7.2+ Jd20
Vd7.2+ Jd33
S1 0 0 1
S2 0 3 1
S3 0 0 3
S4 0 1 0
S5 0 0 3
S6 0 0 0
S7 0 0 0
S8 0 0 0
S9 0 0 0
S10 0 0 2
S11 1 2 8
S12 1 0 6
S13 0 1 0
S14 0 1 1
S15 0 1 0
S16 0 2 4
S17 0 2 2
S18 0 0 7
S19 5 1 30
S20 0 0 0
S21 0 0 0
S22 0 0 0
S23 0 0 0
(C)
Lymphoid Cell Clusters
01 Exhausted T cells
02 Th17–like T cells
03 APC
04 HSP–high
05 Central Memory T cells
06 Cytotoxic T cells
07 HLA II–high
08 Tregs
09 Activated NK cells
10 Effector/Memory T cells
11 ISG–high T cells
12 Resting NK cells
13 Proliferating T cells
UMAP_2
UMAP_1
(D)
CD247
FCGR3A
ITGAM
CD83
NCAM1
ZBTB16
GZMB
PRF1
TBX21
GNLY
KLRD1
XCL1
ITGAE
XCL2
EOMES
IFIT2
IFIT1
HLA–DQA1
CD14
CD68
HSPA1B
IFNG
TOX
MKI67
IL2
IL7R
CD40LG
TXNIP
S100A6
CD3E
LINC01871
GZMK
PDCD1
CD3D
CD3G
LYAR
CD8A
CD8B
AREG
KLRB1
TCF7
CD69
CD4
IL2RA
FOXP3
SELL
LEF1
LTB
CCR7
RORC
GATA3
01 Exhausted T cells
02 Th17–like T cells
03 APC
04 HSP–high
05 Central Memory T cells
06 Cytotoxic T cells
07 HLA II–high
08 Tregs
09 Activated NK cells
10 Effector/Memory T cells
11 ISG–high T cells
12 Resting NK cells
13 Proliferating T cells
(E)
MAIT Positive
MAIT Negative
Proportion
Samples
S16 S18 S3 S12 S2 S5 S17 S14 S10 S19 S11 S15 S21 S22 S23
01 Exhausted T cells
02 Th17–like T cells
03 APC
04 HSP–high
05 Central Memory T cells
06 Cytotoxic T cells
07 HLA2–high
08 Tregs
09 Activated NK cells
10 Effector/Memory T cells
11 ISG–high T cells
12 Resting NK cells
13 Proliferating T cells
(F)
TH17–like
MAIT
UMAP_2
UMAP_1
(G)
RORC
Gene Expression
UMAP_2
UMAP_1

Figure 4.

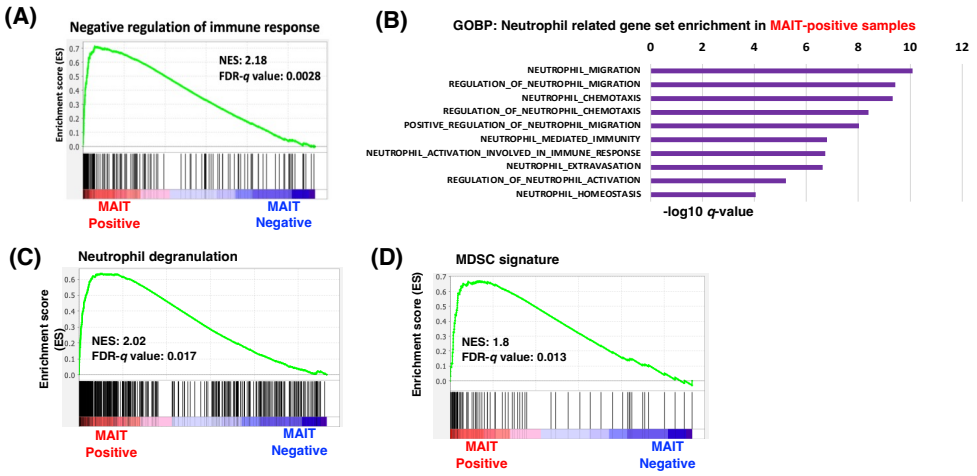
(A)
Negative regulation of immune response
Enrichment score (ES)
NES: 2.18
FDR-q value: 0.0028
MAIT Positive
MAIT Negative
(B)
GOBP: Neutrophil related gene set enrichment in MAIT-positive samples
0
2
4
6
8
10
12
NEUTROPHIL_MIGRATION
REGULATION_OF_NEUTROPHIL_MIGRATION
NEUTROPHIL_CHEMOTAXIS
REGULATION_OF_NEUTROPHIL_CHEMOTAXIS
POSITIVE_REGULATION_OF_NEUTROPHIL_MIGRATION
NEUTROPHIL_MEDIATED_IMMUNITY
NEUTROPHIL_ACTIVATION_INVOLVED_IN_IMMUNE_RESPONSE
NEUTROPHIL_EXTRAVASATION
REGULATION_OF_NEUTROPHIL_ACTIVATION
NEUTROPHIL_HOMEOSTASIS
-log10 q-value
(C)
Neutrophil degranulation
Enrichment score (ES)
NES: 2.02
FDR-q value: 0.017
MAIT Positive
MAIT Negative
(D)
MDSC signature
Enrichment score (ES)
NES: 1.8
FDR-q value: 0.013
MAIT Positive
MAIT Negative

Figure 5.

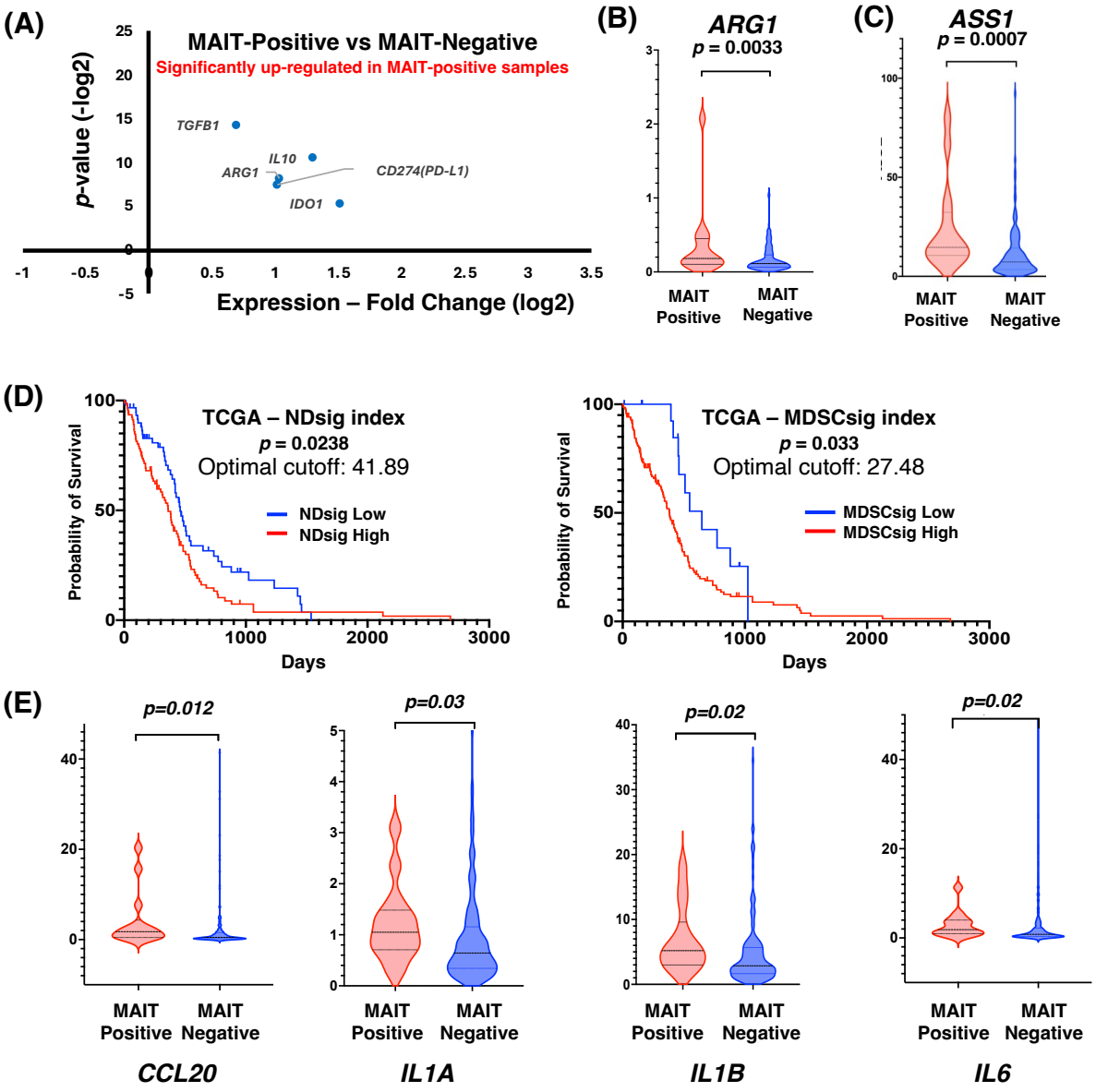
(A)
MAIT-Positive vs MAIT-Negative
Significantly up-regulated in MAIT-positive samples
p-value (-log2)
Expression – Fold Change (log2)
TGFB1
IL10
ARG1
CD274(PD-L1)
IDO1
(B)
ARG1
p = 0.0033
MAIT Positive
MAIT Negative
(C)
ASS1
p = 0.0007
MAIT Positive
MAIT Negative
(D)
TCGA – NDsig index
p = 0.0238
Optimal cutoff: 41.89
NDsig Low
NDsig High
Probability of Survival
Days
TCGA – MDSCsig index
p = 0.033
Optimal cutoff: 27.48
MDSCsig Low
MDSCsig High
Probability of Survival
Days
(E)
p=0.012
CCL20
p=0.03
IL1A
p=0.02
IL1B
p=0.02
IL6
MAIT Positive
MAIT Negative

Figure 6.

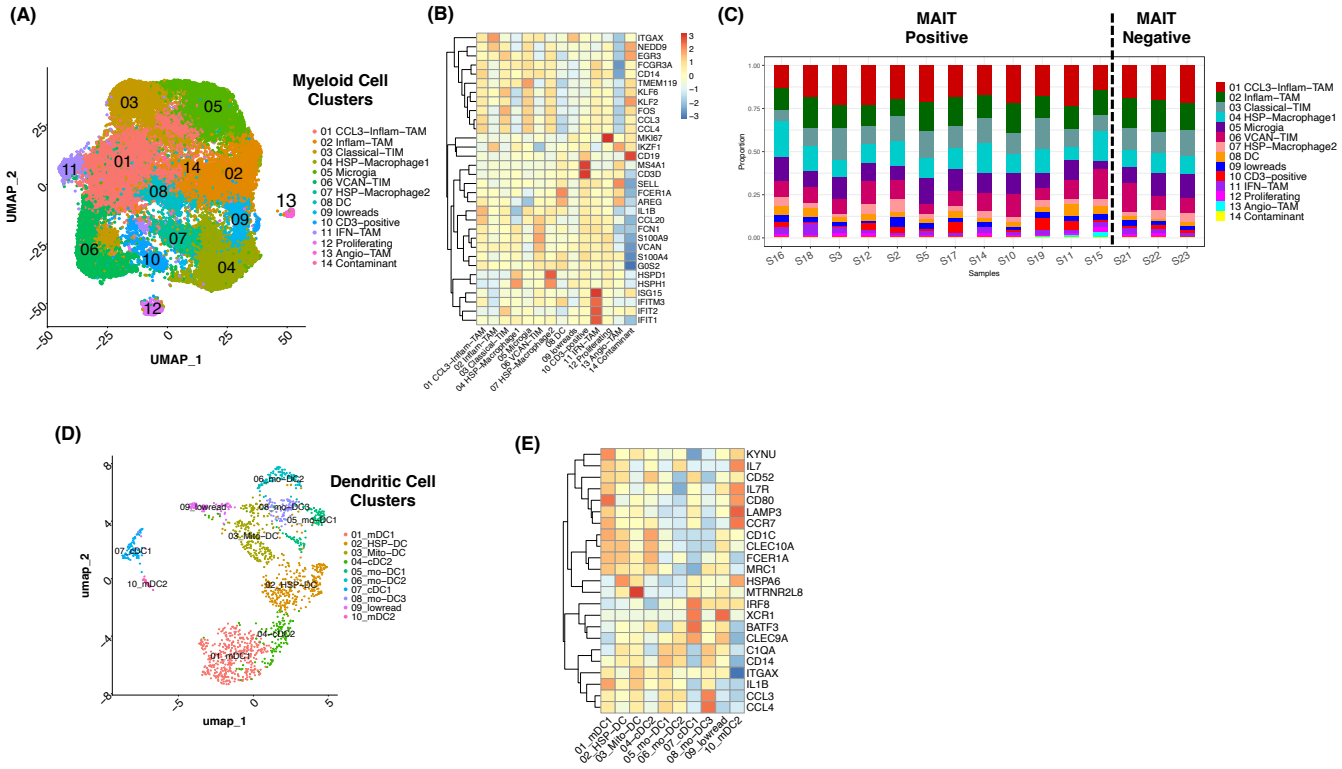
(A)
Myeloid Cell Clusters
01 CCL3–Inflam–TAM
02 Inflam–TAM
03 Classical–TIM
04 HSP–Macrophage1
05 Microgia
06 VCAN–TIM
07 HSP–Macrophage2
08 DC
09 lowreads
10 CD3–positive
11 IFN–TAM
12 Proliferating
13 Angio–TAM
14 Contaminant
UMAP_1
UMAP_2
(B)
ITGAX
NEDD9
EGR3
FCGR3A
CD14
TMEM119
KLF6
KLF2
FOS
CCL3
CCL4
MKI67
IKZF1
CD19
MS4A1
CD3D
SELL
FCER1A
AREG
IL1B
CCL20
FCN1
S100A9
VCAN
S100A4
GOS2
HSPD1
HSPH1
ISG15
IFITM3
IFIT2
IFIT1
(C)
MAIT Positive
MAIT Negative
Proportion
Samples
S16
S18
S3
S12
S2
S5
S17
S14
S10
S19
S11
S15
S21
S22
S23
(D)
Dendritic Cell Clusters
01_mDC1
02_HSP–DC
03_Mito–DC
04–cDC2
05_mo–DC1
06_mo–DC2
07_cDC1
08_mo–DC3
09_lowread
10_mDC2
umap_1
umap_2
(E)
KYNU
IL7
CD52
IL7R
CD80
LAMP3
CCR7
CD1C
CLEC10A
FCER1A
MRC1
HSPA6
MTRNR2L8
IRF8
XCR1
BATF3
CLEC9A
C1QA
CD14
ITGAX
IL1B
CCL3
CCL4

Figure 7.

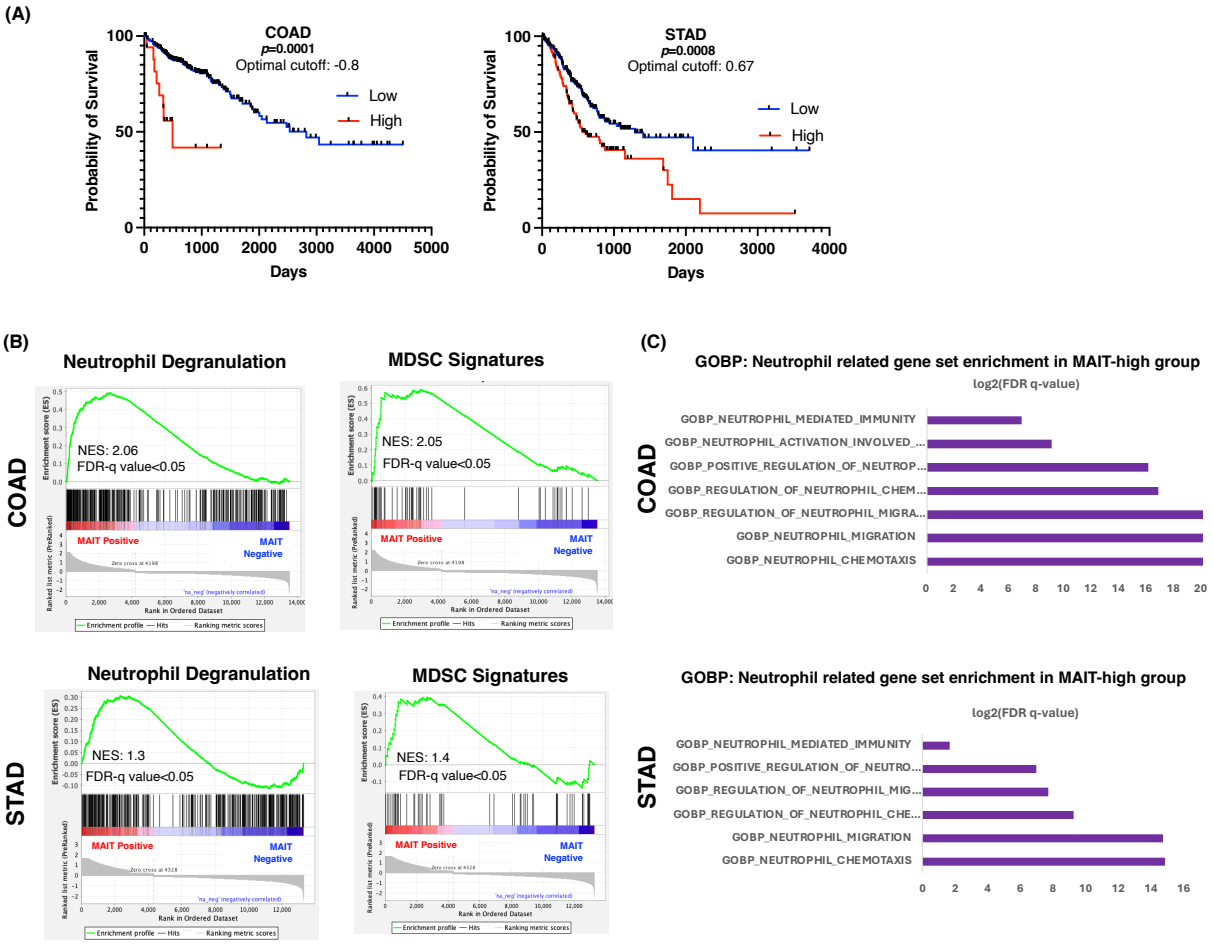
(A)
COAD
p=0.0001
Optimal cutoff: -0.8
Low
High
Probability of Survival
Days
STAD
p=0.0008
Optimal cutoff: 0.67
Low
High
Probability of Survival
Days
(B)
Neutrophil Degranulation
MDSC Signatures
COAD
NES: 2.06
FDR-q value<0.05
NES: 2.05
FDR-q value<0.05
MAIT Positive
MAIT Negative
STAD
NES: 1.3
FDR-q value<0.05
NES: 1.4
FDR-q value<0.05
(C)
GOBP: Neutrophil related gene set enrichment in MAIT-high group
log2(FDR q-value)
GOBP_NEUTROPHIL_MEDIATED_IMMUNITY
GOBP_NEUTROPHIL_ACTIVATION_INVOLVED_...
GOBP_POSITIVE_REGULATION_OF_NEUTROP...
GOBP_REGULATION_OF_NEUTROPHIL_CHEM...
GOBP_REGULATION_OF_NEUTROPHIL_MIGRA...
GOBP_NEUTROPHIL_MIGRATION
GOBP_NEUTROPHIL_CHEMOTAXIS
GOBP_NEUTROPHIL_MEDIATED_IMMUNITY
GOBP_POSITIVE_REGULATION_OF_NEUTRO...
GOBP_REGULATION_OF_NEUTROPHIL_MIG...
GOBP_REGULATION_OF_NEUTROPHIL_CHE...
GOBP_NEUTROPHIL_MIGRATION
GOBP_NEUTROPHIL_CHEMOTAXIS

Figure 8.

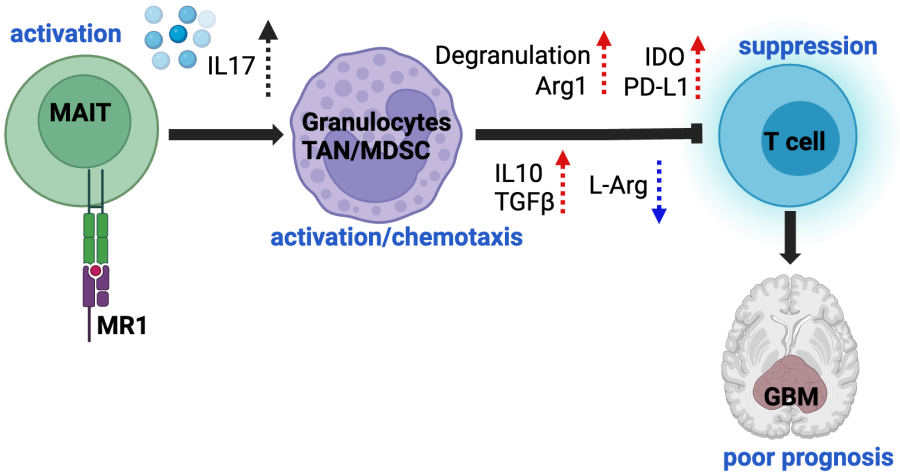
activation
IL17
MAIT
MR1
Granulocytes
TAN/MDSC
activation/chemotaxis
Degranulation
Arg1
IDO
PD-L1
IL10
TGFβ
L-Arg
suppression
T cell
GBM
poor prognosis